RSC Advances

ROYAL SOCIETY OF CHEMISTRY

www.rsc.org/advances

Improved microwave absorption in light weight resin based carbon foam by decorating with magnetic and dielectric nanoparticles

R. Kumar[1], A. P. Singh[1], M. Chand[2], R. P. Pant[2], R. K. Kotnala[1], S. K. Dhawan[1], R. B. Mathur[1], S. R. Dhakate[1]*

[1]Division of Material Physics and Engineering, CSIR-National Physical Laboratory
[2] EPR Section, CSIR-National Physical Laboratory,
Dr. K. S. Krishnan Marg, New Delhi 110012 (India)

Abstract

Carbon foams (CFoam) are sponge-like high performance light weight engineering materials possess excellent electrical and mechanical properties as well as thermal stability. The CFoam possess bulk density in the range 0.30 to 0.40 g.cm^{-3} and open porosity more than 70 %. In CFoam pore walls i.e., ligaments, are interconnected to each other, that are responsible for the conduction path and hence the electrical conductivity due to mobile charge carrier (delocalized π electron). The high value of electrical conductivity causes the CFoam as an electromagnetic radiation reflector rather than absorber. While in certain application shielding materials have mandatory to absorb maximum electromagnetic radiation. Therefore, to improve the absorptivity of electromagnetic radiation in light weight CFoam, the CFoams are decorated by Fe_3O_4 and ZnO nanoparticles. It is observed that Fe_3O_4 and Fe_3O_4 -ZnO nanoparticles coating not only improved the absorption losses but also enhanced the compressive strength of CFoam by 100%. The CFoam demonstrate excellent shielding response in the frequency range 8.2 to 12.4 GHz in which total shielding effectiveness(SE) dominated by absorption losses. The total SE is -45.7 and -48.5dB of Fe_3O_4 and Fe_3O_4- ZnO coated CFoam, it is governed by absorption losses -34.3 dB and -41.5 dB. The absorption losses increases by 236 % in Fe_3O_4 coated CFoam and 281 % in Fe_3O_4-ZnO coated CFoam without much enhancement in the bulk density of it. This is due to the high level of magnetic and dielectric losses of nanoparticles with high surface area. The absorption losses are 80 % higher than any reported value of CFoam. Thus light weight CFoam decorated with magnetic and dielectric nanoparticles is excellent material for stealth technology.

*Corresponding author Email: dhakate@mail.nplindia.org, Tel: 0911145608257, Fax: 091145609310

1. Introduction

In the recent time considerable interest generated in the realization of innovative electromagnetic (EM) absorbing materials that are even more lightweight and have multifunctional properties. Particularly, EM radiation absorbing materials have gained lot of interest in civil and military applications such as in stealth technology, reduction of radar signature of aircrafts, ships, tanks etc. Stealth technology allows an aircraft to be partially invisible to radar or any other means of detection.[1,2] This doesn't allow the aircraft to be fully invisible on radar. This is similar to the camouflage tactics used by soldiers in jungle warfare. The different metals and their nanoparticles have been explored in the recent time but they have drawbacks of high density, corrosion, difficult/uneconomic processing and low specific shielding capability.[3] Among different materials for civil and military applications, carbon based materials have gained popularity because of their high electrical/thermal conductivity, low density, good corrosion resistance, thermal stability and processing advantages.[4] The carbon material properties can be tailored by controlling processing parameters. Carbon based shielding materials not only protect from EM radiations but also control regulation of thermal heating in electronic power systems to protect them from any form of damage or catastrophe. Therefore, technologists and scientists are looking for highly efficient, thermally conducting and lightweight radar absorbing material (RAM) particularly for aerospace transportation vehicles in civil, military and space structure applications. The shielding materials should not only have strong microwave absorption properties but should also be lightweight and cost-effective.[5]

Recently, light weight carbon foam (CFoam) has emerged as a promising candidate for different applications owing to its outstanding properties such as low density, large surface area with open cell wall structure, good thermal/electrical transport properties and mechanical stability.[6,7]The CFoams are sponge-like high performance engineering materials in which carbon ligaments are interconnected to each other, and have recently attracted attention due to their potential applications in various fields.[8]The CFoam is generally developed from thermosetting and thermoplastic polymers by

various techniques.[9-12] The thermosetting polymer i.e. phenolic resin derived CFoam is less electrically and thermally conductive.[13-15] While coal tar pitch and mesophase pitch derived CFoams are thermally and electrically conductive.[16,17]In both the cases EM shielding effectiveness (SE) is dominated by reflection losses rather than absorption losses due to the high electrical conductivity value of CFoam.[18,19]

In the open literature few studies on CFoam are available in which CFoam are heat treated in between temperature 400-800°C.[20-27] Yang et al [20] reported the development of CFoam from mesophase pitch by foaming technique and studied its microwave (2-18 GHz) absorption characteristics. It is found that CFoam heat treated at 600 and 700°C exhibit better microwave absorption (reflection loss 10 dB). Fang et al [22] has reported electromagnetic characteristic of CFoams having different pore size and electrical conductivities which are controlled by carbonization temperature (700-760°C). The electromagnetic parameters of these CFoam and their corresponding pulverized powders are measured by a resonant cavity perturbation technique at a frequency of 2.45 GHz. The CFoam has dielectric loss several times larger than their corresponding pulverized powder. Recently, Moglie et al [23] studied the EM SE of CFoam (GRAFOAM FPA-20 and FRA-10) in the frequency band 1-4 GHz using the nested reverberation chamber method. It is reported that with increasing thickness of CFoam Total SE increases. Micheli et al[24] reported the effect of multi walled carbon nanotubes epoxy resin mixture filled in the pores of CFoam and studied its role on EM radiation absorption properties of CFoam in frequency range 2-3 GHz. It is found that reflection coefficient reaches up to –45 dB. Blacker et al [25] reported EM SE (40dB) in the frequency range of 400 MHz -18 GHz of rigid porous electrically conductive CFoam, in which electrically conductive carbon nanofiber polymer matrix is used for the joining the CFoam enclosures. Blacker et al [26], reported the development of electrically graded CFoam material and its electrical resistivity increases with increasing the thickness and decreases with increasing processing temperature. These electrically graded CFoam can be used as radar absorbers. Kuzhir et al [27], reported the EM SE of CFoam

developed from commercial tannin and furfuryl alcohol which is pyrolysed at 900°C. The absorption and reflection of EM SE in microwaves are depending on the density of CFoam. The maximal SE value is 23 dB in Ka band (26-40 GHz) achieved for the density (0.150 g/cm^3) of CFoam.

The microwave absorption in shield material is due to the different interactive energy dissipation processes of polarization and magnetization.[28] Therefore, in the present study to improve the microwave absorption in CFoam derived from phenolic resin are coated with magnetic ferrofluid and dielectric zinc oxide nanoparticles. The resultant CFoams are characterized by Scanning electron microscopy, Transmission electron microscope, Raman microscopy, X-ray diffraction, vibration sample magnetometer and vector network analyzer.

2. Experimental section

2.1. Development of Carbon Foam

Thermosetting phenolic resin based CFoams were prepared by sacrificial template route by impregnating phenolic resin into the commercially available PU foams. The PU foams of density 0.030 g.cm^{-3} of cell sizes 0.45 mm and cell numbers per unit length 50 pores per inch was used to develop the CFoam. The solution of phenolic resin 40 wt.% and organic solvent was prepared to impregnate PU foam. The porous PU foam slabs were cleaned with acetone and dried for 15 minutes followed by drying in hot oven for 2 hrs. The dried foams were impregnated by resin solution at room temperature. The impregnation was carried out carefully by removing excess resin solution in order to avoid retention of resin into the pores of substrate foam resulting in uniform structure in the final product. Impregnated foams were dried at 60°C for 12 hrs. The dried resin impregnated foams were cured at 150°C in presence of air atmosphere for 12 hrs for increasing the cross-linking between the polymeric chains. These cured foam slabs were pyrolysed at 500°C for 1 hr and later on carbonized at 1000°C in inert atmosphere to get the CFoam. The resulting carbonized foam was denoted as CFoam C1.

The CFoam C1 coated with magnetic (Fe_3O_4) and dielectric ZnO nanoparticles to improve the radar emission absorptivity i.e. electromagnetic radiation can be absorbed by material. In first case CFoam C1 was coated with ferrofluid solution using dip coating and it is denoted as CFoamC2. The ferrofluid was a colloidal suspension of Fe_3O_4 nanoparticles. In another case CFoam C1 coated with ferrofluid and ZnO nanoparticles and it is denoted as CFoamC3. The ZnO nanoparticles are prepared by thermal evaporation of zinc acetate [29] at 60-70°C at slow heating. After coating of nanoparticles, these CFoams were heat treated at 650°C for 10 minute in inert atmosphere. In case CFoam C2, loading of the Fe_3O_4 nanoparticles was 14 wt % and in case C3, Fe_30_4 and ZnO loading is 7 wt % each with respect to weight CFoam. The CFoams were characterized by different techniques for evaluation of radar emission absorptivity.

2.2 Characterization

Raman spectra of the CFoam samples were recorded using Renishaw in Via Raman spectrometer, UK with laser as an excitation source at 514 nm. The crystal structure of CFoam samples were studied by X-ray diffraction (XRD, D–8 Advanced Bruker diffractometer) using CuK_α radiation (λ = 1.5418 Å). The surface morphology of the CFoam samples was observed by scanning electron microscope (SEM, VP-EVO, MA-10, Carl-Zeiss, UK) operating at an accelerating potential of 10.0 kV. The electrical conductivity CFoam (size 60 mm x 20 mm x 4 mm) was measured by d.c. four probe contact method using a Keithley 224 programmable current source for providing current. The voltage drop was measured by Keithley 197A auto ranging digital microvoltmeter. The values reported in text are average of six readings of voltage drops at different portions of the sample. EM-SE and EM attributes (complex permittivity and permeability) was measured by waveguide using vector network analyzer (VNA E8263BAgilent Technologies). The rectangular samples of thickness 2.75 mm were placed inside the cavity of sample holder which matches the internal dimensions of X-band (8.4–12.4 GHz) wave guide. The sample holder was placed between the flanges of the waveguide connected between

the two ports of VNA. The magnetic property of the CFoam samples were measured by vibration sample magnetometer (VSM) model 7304, Lakeshore Cryotronics Inc., USA with a maximum magnetic field of 1.2T, vibrating horizontally at frequency 76 Hz.

2. Results and Discussion

2.1 Electrical conductivity of CFoams

The CFoam C1 developed by sacrificial template technique from thermosetting phenolic resin possesses bulk density 0.34 $g.cm^{-3}$. The coating of Fe_3O_4 particles CFoam, increases bulk density of CFoam C2 from 0.34 $g.cm^{-3}$ to 0.40 $g.cm^{-3}$. Further, the CFoam C1, coated with mixture of Fe_3O_4-ZnO nanoparticles (CFoam C3), the density is almost same as CFoam C2. The attenuation of microwave is depends upon the electric and magnetic properties of CFoam. In this direction electrical conductivity of all the CFoam measured and it is reported in Table 1. The electrical conductivity of CFoam C1 is 20 $S.cm^{-1}$ because foam derived from the phenolic resin possesses higher conductivity due to the delocalized π electron in the carbon network but is comparatively very less as compared to pitch based carbon foam.[30] However, Fe_3O_4 coated CFoam C2 electrical conductivity decreases to 13 $S.cm^{-1}$. Further on mix coating of Fe_3O_4-ZnO (CFoam C3), the electrical conductivity is almost same with the conductivity of CFoam C2. The decrease in conductivity is due to the Fe_3O_4 and ZnO inhibit in the conduction path of electrons. The interactions between conducting CFoam and Fe_3O_4-ZnO particles during heat treatment at temperature 650ºC, form the complex which can reduced the conductivity, also coating of magnetic and dielectric nanoparticles on the surface of CFoam increases the contact resistance which can inhibit conduction path.

Table 1: Properties of Carbon foam

CFoam	Bulk Density ($g.cm^{-3}$)	Electrical Conductivity ($S.cm^{-1}$)	Thermal Conductivity ($W.m^{-1}.K^{-1}$)	Compressive Strength (MPa)
C1	0.34	20.00	0.54	4.00
C2	0.40	14.00	-	7.00
C3	0.40	13.50	-	8.00

The Fe_3O_4 and ZnO nanoparticles coating on CFoam have positive effect on the mechanical properties. The strength is one of the essential requirements of CFoam because compressive forces are often encountered during service life. Therefore, compressive strength of CFoam should be sufficient to avoid any form of structural damage. The compressive strength of CFoam depends mainly on two factors namely microstructure and bulk density. It is observed that the compressive strength of CFoamC1 is 4.0 MPa and that of Fe_3O_4 coated CFoam C2 is 7 MPa. While Fe_3O_4-ZnO coated CFoam C3 strength is 8 MPa. This enhancement in strength is related to increase in bulk density and decrease in stress concentration centre as the coating might reduced the number of crack in CFoam. In the shield material heat is generated due to the absorption of EM radiations, therefore CFoam should have sufficient thermal conductivity for heat dissipation. The thermal conductivity of CFoam is measured by laser flash method and it is 0.54 $W.m^{-1}. K^{-1}$.

2-2 Morphology of CFoam

In Figure 1 depicted the SEM micrographs of Polyurethane template foam, CFoam C1, C2 and C3. The Polyurethane template foam possesses different size and shapes of cells (figure1a), which are connected by thin wall. While in case CFoam C1, cells of the different sizes and distributions of cells are not uniform (figure1b). In CFoam cells are mainly open with incomplete cell membrane and each cell is sealed off from its neighbors cell partly i.e., ligaments. While in Fe_3O_4 coated CFoam C2 (Figure 1c), stresses exerting on the cell membrane during heat treatment at 650ºC and as a results cells are open but on the other hand cracks are developed in Fe_3O_4 coated ligaments (Figure 1d, magnified view of cell wall) due to the differential thermal expansion of CFoam and Fe_3O_4 nanoparticles. The ferrofluid consist of Fe_3O_4 nanoparticles of size between 50-100 nm and after coating on the CFoam it will get agglomerated (Supplementary information Figure S1 a & b). Also depicted in Figure 1d, crack developed on the surface of CFoam in coating area and which are maximum on pore walls or ligaments (Supplementary information Figure S1c). Figure 1e shows SEM image CFoamC3 coated

with Fe_3O_4 -ZnO nanoparticles. As observed in Figure 1c, the Fe_3O_4 particles coated on surface of the ligaments of CFoam while in case of CFoamC3, Fe_3O_4 is coated on the ligaments and ZnO nanoparticles impregnated inside the pores.

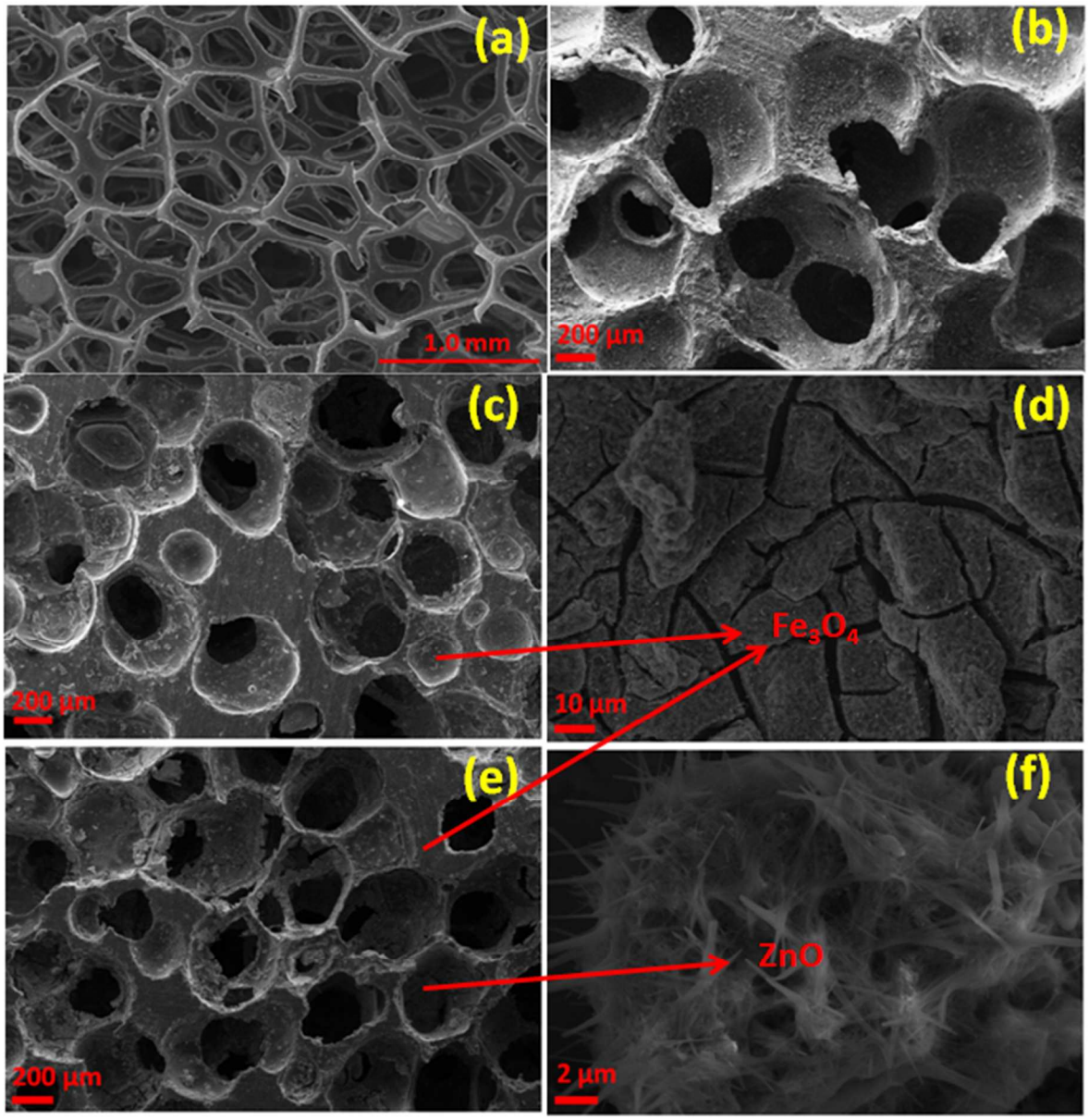

Figure 1: SEM images of (a) Polyurethane template Foam, (b) CFoam C1, (c) CFoam C2 coated with Fe_3O_4, (d) CFoam C2 in which cracks generated after heating, (e) CFoam C3 coated with Fe_3O_4-ZnO**,** (f) ZnO nanorods generated inside the pores of CFoam C3.

The evolution of in-situ ZnO nanorods in the pores after heat treatment at 650°C of CFoam is shown in Figure 1 (e and f). The ZnO nanoparticles synthesized by thermal evaporation of zinc acetate at low

temperature 60-70 °C and morphology of ZnO nanoparticles is shown in supplementary information (FigureS2a). The ZnO nanoparticles with ferrofluid solution coated on CFoam and heat treated at 650°C. The Fe_3O_4 coated on the mostly on the surface of CFoam while some Fe_3O_4 nanoparticles and ZnO impregnated mostly in the pores of CFoam. After heat treatment it is observed that flower type morphology of ZnO and Fe_3O_4, inside the pores shown in supplementary information (Figure S2b, c and d). From the transmission electron microscopy (TEM) image of ZnO nanoparticles, it is observed that ZnO nanoparticles have an average diameter of 70 nm. At higher magnification, in nano-rod have fringe type structure is repetitively observed, this evident that during heat treatment of ZnO particles transform into nano-rod like structure (Figure 1f).

2.3 X ray diffraction and Raman spectra of CFoams

Figure 2 shows the XRD pattern of CFoam C1, C2 and C3. The CFoamC1 is carbon derived from the phenolic resin consist of two peaks at 2θ equal to 24.1^{O} and 44.4^{O} are correspond to the amorphous carbon of 002 and 101 lattice plane. The CFoamC2 is Fe_3O_4 coated, it consist of peaks of amorphous carbon and Fe_3O_4 at 2θ equal to 29.18^{O}, 35.1^{O}, 43.26^{O}, 44.6^{O}, 57.15^{O} and 62.55^{O}. The XRD pattern of magnetic nanoparticles (Fe_3O_4) is given in supplementary information (Figure S4). During the heat treatment, interactions between the carbon and Fe_3O_4 nanoparticles occur at temperature between 500-650^{o}C, which form Fe-C. It is well known that carbon is a reducing agent which can react with Fe-O compounds during heat treatment and compounds Fe-O transform into iron carbide.[31] Also the peaks of Fe_3O_4 are shifted to lower diffraction angle, this suggest that successful incorporation of dopant in the host matrix.

While in case of CFoam C3, it is observed that ZnO and Fe_3O_4 are coexisting with carbon, which results in to the change in the peak position that has positive effect on the magnetic properties of the CFoams. Therefore, CFoam C3 consists of peaks amorphous carbon, Fe_3O_4 and ZnO at 2θ equal to

24.70°, 29. 26°, 31.66°, 34.46°, 36.22°, 44.626°, 47.42°, 56.43°, 62.876°, 64.95°, 67.958° and 75.32°. In figure S4 given X-diffraction pattern of ZnO(supplementary information). The spectra consist of peaks at 2θ equal to 31.8°, 34.5°, 36.4°, 47.6°, 56.4°, 62.9°, 68.0° are corresponds to 100,002,101,102,110, 103, 200 lattice planes of wurtzite ZnO structure. [32]

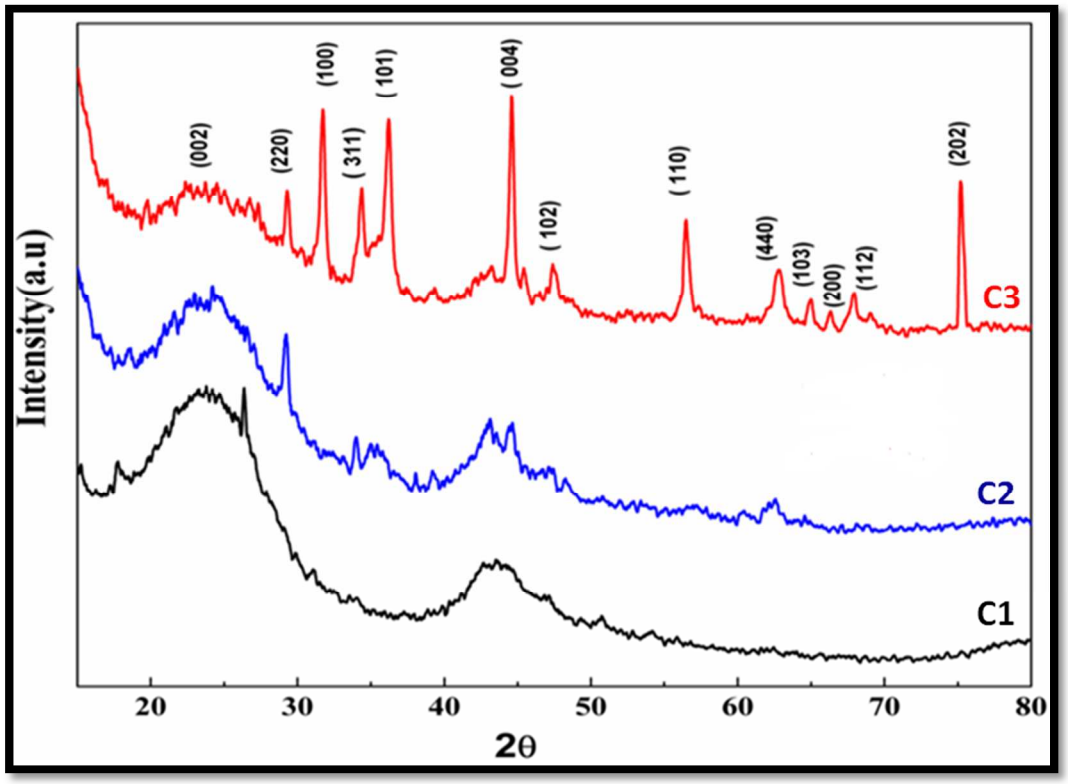

Figure 2: X-ray diffraction pattern of CFoam C1, C2 and C3.

Figure3a shows the Raman spectra of CFoam C1, C2 and C3 in the range of Raman shift 1000-3000 cm^{-1}. The Raman spectra illustrate common features in the Raman shift 1000-3000 cm^{-1}region, the G, D and 2D band which lies at around 1560, 1360 and 2700 cm^{-1} respectively. The G band corresponds to the E_{2g} phonon at the Brillion zone centre. The D band is due to the breathing modes of sp^2 atoms and requires a defect for its activation and it only gives knowledge to the amount of disorder in the given structure.[33,34] In this investigation the CFoam is derived from the phenolic resin which is heat treated at 1000ºC and it gives hard carbon which is in amorphous nature. The spectra of CFoamC1

consist of D and G band peak at 1349 and 1597 cm^{-1} while in case CFoam C2 and C3 peak appears at almost same Raman shift (1348 and 1601 cm^{-1}) but intensity is different. The intensity ratio of D and G (ID/IG) peak gives idea of defect level in the structure of CFoam .i.e. sp^3 bonded carbon. The higher is ID/IG ratio of CFoam, lesser amount of sp^2 bonded carbon i.e., more defects the structure.

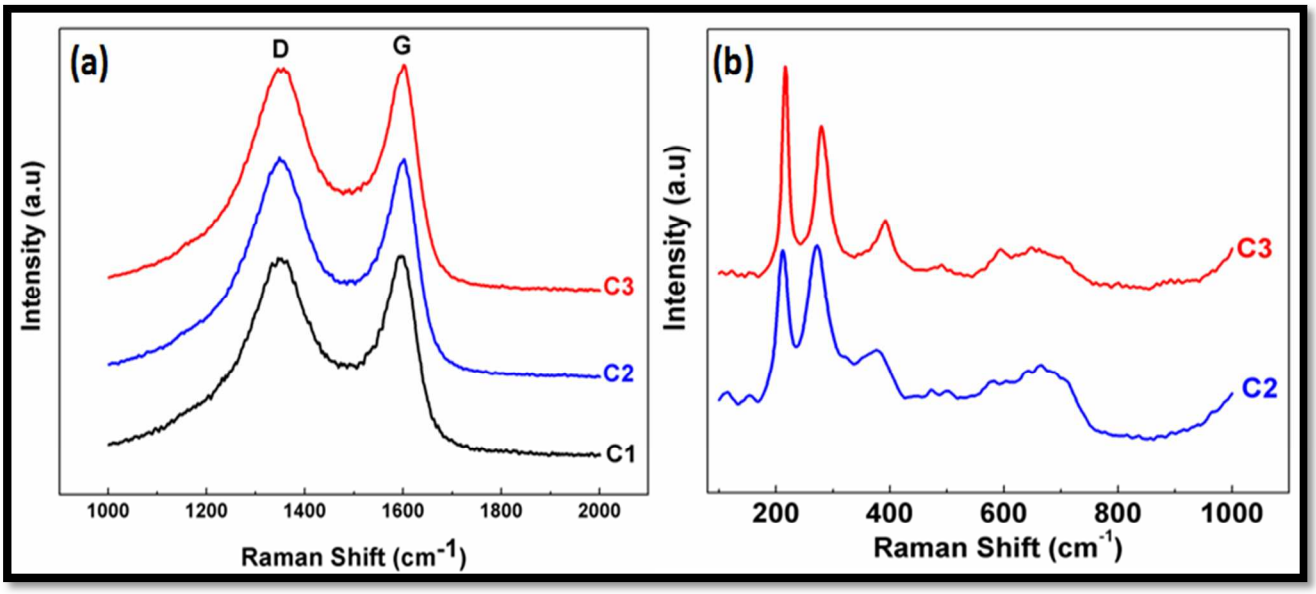

Figure 3: (a) Raman Spectra of CFoam C1, C2 and C3, **(b)** Raman Spectra of CFoam C2 and C3 in the Raman shift range (100-900 cm^{-1})

The CFoam C1 has the ID/IG ratio 0.955 while in case of C2 and C3 it increases to 1.03. This demonstrate that the Fe_3O_4 and ZnO coating form the complex with sp^3 carbon and as a consequence increase in value of ID/IG ratio and decrease in the value of electrical conductivity of C2 and C3. The decreases in electrical conductivity due to the increases in defect level in CFoam that can influence the shielding effectiveness of the CFoam C2 and C3. As a result increases in the absorption component and decreases in the reflection component of total SE of the CFoam C2 and C3. Hence, total shielding effectiveness increases due to the higher contribution of absorption component. The Raman spectra in the range of 200-1000 cm^{-1} of CFoam are depicted in Figure 3b, in this region peak appears is related to Fe_3O_4 and ZnO nanoparticles. In case of Fe_3O_4 coated CFoamC2 peaks registered at Raman

shift 215, 280, 380, 422, 496, 663 and peak between 710-720 cm $^{-1}$ is clearly evident of the magnetite nano crystals (Fe_3O_4) with the surface partially oxidized to maghemite.[29,35] However, in case of the Fe_3O_4 and ZnO coated CFoamC3 peaks ~340,442, 580 cm^{-1} are of ZnO nanoparticles registered in addition to the peaks of Fe_3O_4. Raman active zone-center optical phonons predicted by the group theory are $A1+ E1+ 2E2$. The phonons of $A1$ and $E1$ symmetry are polar phonons and hence exhibiting different frequencies for the transverse-optical (TO) and longitudinal-optical (LO) phonons. Nonpolar phonon modes with symmetry$E2$ have two frequencies. $E2$H is associated with oxygen atoms and $E2$L is associated with Zn sub lattice. The presence of sharp $E2$H (442 cm^{-1}) mode with high intensity and the second-order Raman mode at 340cm^{-1} in the Raman spectra indicates that obtained sample possesses the wurtzite ZnO. According to the theory of polar optical phonons wurtzite nanocrystals, the wave number of LO phonon mode in ZnO should be in between 574 and 591cm^{-1}.

2.4 Permittivity and Magnetic permeability of CFoam

Figure 4 shows the EM attributes, relative complex permittivity ($\varepsilon^*=\varepsilon'-i\varepsilon''$) and relative complex permeability ($\mu^*=\mu'-i\mu''$) of CFoam measured in the frequency region 8.2 -12.4 GHz to correlate with microwave shielding properties of CFoams. These complex parameters have been estimated from experimental scattering parameters (S_{11}& S_{21}) by standard Nicholson-Ross and Weir theoretical calculation [36,37]. The estimated real part of the EM parameters (ε', μ') is directly associated with the amount of polarization occurring in the material which symbolizes the storage ability of the electric and magnetic energy, while imaginary part (ε'', μ'') is signifies the dissipated electric and magnetic energy. From Figure 4 (a and b) it clearly demonstrates that both real and imaginary part of the permittivity (ε', ε'') varies with frequency in all the type CFoams. The real permittivity in CFoam C2 and C3 decreases with increasing the frequency while in CFoamC1 exhibit a broad peak in the frequency region 9.5 -10.5 GHz which reveals the resonance behaviour due to the high value of electrical conductivity (Figure 4a).

Furthermore, skin effect becomes significant [38] in CFoam due to its high surface area and high value of conductivity. The decreasing permittivity in C2 and C3 with frequency could be ascribed to the decreasing capability of the dipoles to sustain the in-phase movement with speedily pulsating electric vector of the incident radiation. The real permittivity at fixed frequency 10 GHz is 90, 40 and 15 for CFoam C1, C2 and C3 respectively.

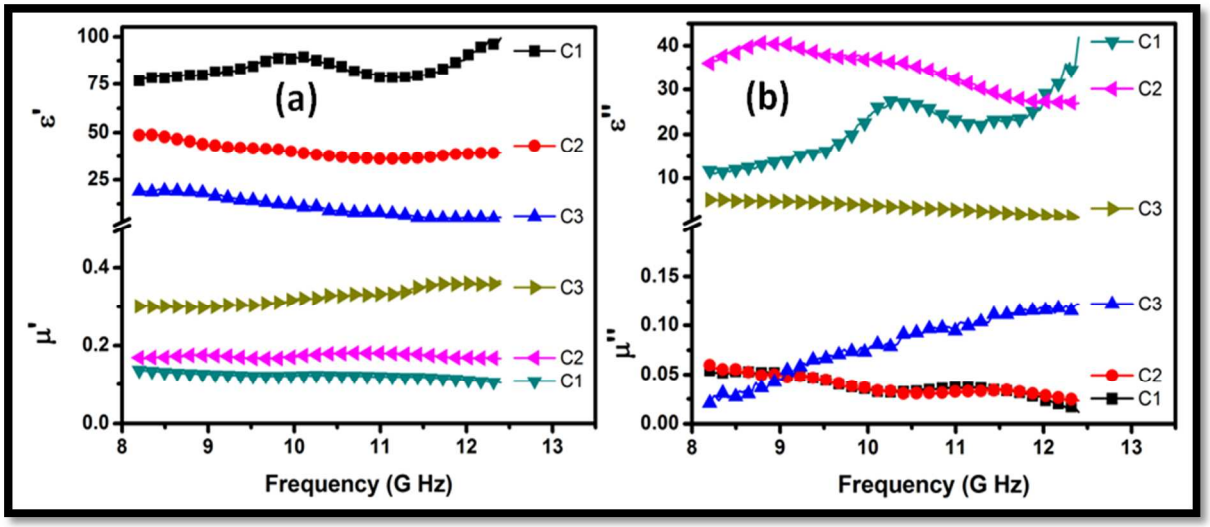

Figure 4: (a) Real permittivity and permeability (ε′,μ′), (b) imaginary permittivity and permeability ((ε″,μ″) of CFoam C1, C2 and C3.

According to EM theory [39.40], the ac conductivity (σ_{ac}) and skin depth (δ) are related to the imaginary permittivity (ε"), frequency (ω) and real permeability (μ') as $\sigma_{ac} = \omega\varepsilon_o\varepsilon''$, ($\sigma = \sigma_{ac} + \sigma_{dc}$) and $\delta = \sqrt{2/\sigma_{AC}\omega\mu'}$ which gives reflection (SE_R) and absorption loss (SE_A) as:

Reflection loss (SE_R) as

$$SE_R(dB) = 10\log\{\sigma_{ac}/16\omega\varepsilon_0\mu'\} \quad \text{.....(I)}$$

and absorption loss (SE_A) as

$$SE_A(dB) = 20\{t/\delta\}\log e = 20d\sqrt{\mu\omega\sigma_{ac}/2}\log e = 8.68\{t/\delta\} \quad \text{.....(II)}$$

$$SE_A(dB) = 8.68t\sqrt{\sigma\omega\mu'/2} \quad \text{.....(III)}$$

From the equation (I), it deduce that SE_R is related to frequency (ω), conductivity (σ_{ac}) and real permeability while the ac conductivity ($\sigma_{ac} = \omega\varepsilon_o\varepsilon''$) is depends upon the frequency and imaginary permittivity (ε"). As shown in figure 4a, real permeability increases with increasing the frequency and it is maximum in case of CFoam C3 and minimum in C1.while imaginary permittivity (Figure 4b) is also varies with frequency and it is minimum in case of CFoam C3. This clearly demonstrates that SE_R is minimum in cases of CFoam C3 and maximum in CFoam C1.

The SE_A is related to thickness, real permeability, frequency and conductivity, from the figure 4, maximum real permeability is in case Fe_3O_4 –ZnO coated CFoam C3 followed by C2 and minimum in C1where thickness is same in all the cases.

The coating of Fe_3O_4 and ZnO nanoparticles on conducting CFoam C1, electrical conductivity decreases in case of CFoamC2 and C3 leading to reduction of imaginary permittivity. The higher value of imaginary component of permittivity, larger is the loss in the shied material. A material with low dielectric loss can store energy, but will not dissipate the stored energy. The material with high dielectric loss does not store energy efficiently and larger part of the energy of the incident wave is converted into heat within the shield material. Therefore, materials with lower value of conductivity yield in to large amount of losses that inhibits the propagation of EM radiation i.e., absorption losses are more in case of CFoam C3. Thus, higher value of real permeability is also responsible for the radiation absorption in CFoam C3. In CFoam, the existence of interfaces between Fe_3O_4 nanoparticles-CFoam, ZnO nanorods-CFoam, and Fe_3O_4-ZnO are responsible for interfacial polarization which further contribute to dielectric losses. Interfacial polarization occurs in heterogeneous media due to the accumulation of charges at the interfaces and the formation of large dipoles. Ferromagnetic nanoparticles act as tiny

dipoles which get polarized in the presence of EM field and as a result better microwave absorption.

The real permeability value of CFoam C3 is more as compared to than that of CFoam C2 and C1 (Figure4a). This is due to the improvement of magnetic properties along with the parallel reduction of eddy current losses since coating material of ferromagnetic behaviour. In the microwave ranges, the natural resonances in the X-band can be attributed to the small size of Fe_3O_4 nanoparticles and ZnO nanorods in the CFoams. Anisotropy energy of the small size materials, especially in the nanoscale, would be higher due to the surface anisotropic field effect of smaller material.[41] The higher anisotropy energy is also contributed in the enhancement of the microwave absorption. The real and imaginary part of complex permeability increases with frequency in CFoam C3 and maximum at frequency 12.4 GHz. While in CFoam C2 and C1, it slightly decrease with the frequency (Figure 4b). This has positive effect on absorption of microwave radiation. The magnetic and dielectric coating on the surface of the CFoam (C2 and C3) leads to better matching of input impedance along with the reduction of skin depth. This is attributing further in the increase of absorption losses of CFoam. This fact also varied by the measuring the saturation magnetization of the CFoam C1, C2 and C3.

3.5 Magnetic properties of CFoam

Figure 5 shows the room temperature magnetization plot of CFoam C1, C2 and C3.The data of magnetization reveals that CFoam C1 does not show any magnetization though out the magnetic field because carbon is nonmagnetic with high electrical conductivity due to the delocalized π electron. However, Fe_3O_4 coated CFoam C2 and Fe_3O_4- ZnO coated CFoam C3 display narrow hysteresis loop.

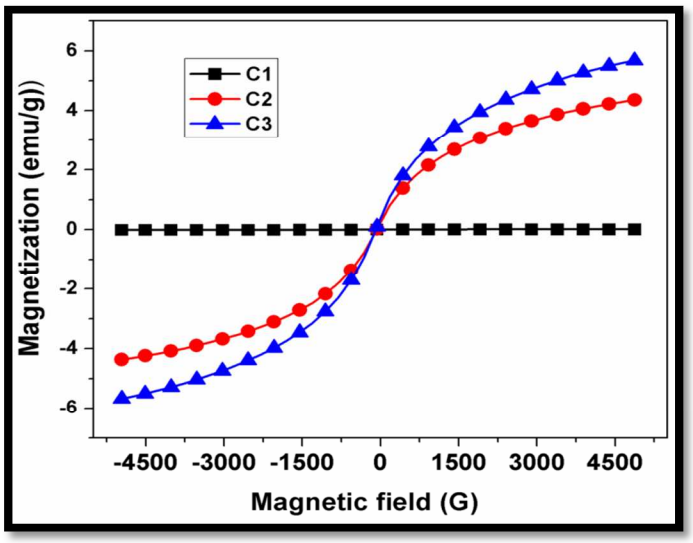

Figure 5: The room temperature magnetization plot of CFoam C1, C2 and C3.

The CFoam C2 possesses saturation magnetization 4.2 emu/g at 4.9 KG while in CFoamC3 saturation magnetization is 5.8 emu/g. The improved saturation magnetization in case of CFoamC3 is due to the addition of ZnO in Fe_3O_4 can also contribute in magnetization. The ZnO doped by Fe_3O_4 and as a consequence ZnO becomes ferromagnetic due to the interaction between zinc oxide and ferrous oxide which form its complex Zn-FeO.[32,42] This can increases the overall magnetic properties of CFoam C3.These results are in agreement with results of electromagnetic attributes. This clearly demonstrate that even small uptake of nanoparticles coating on the conducting CFoam is very much effective for absorption of radar emission due to its large surface area and its properties.

3.6 Electromagnetic shielding and microwave absorbing properties

The validation of microwave shielding can be elucidating by measuring shielding effectiveness (SE) in terms of reflection and absorption losses. The SE of any shield is the ability to attenuate electromagnetic (EM) radiation that can be expressed in terms of ratio of incoming (incident) and outgoing (transmitted) power [43]. The EM attenuation offered by a shield may depend on the three mechanisms: reflection of the wave from the front face of shield, absorption of the wave as it passes through the shield and multiple reflections of the waves at various interfaces [44]. Therefore, SE is

attributed to three types of losses i.e. reflection loss (SE_R), absorption loss (SE_A) and multiple reflection losses (SE_M) and can be expressed (equation I) as:

$$SE_T(dB) = SE_R+SE_A+SE_M = 10\log (P_t/P_i)\text{……(I)}$$

where Pi and Pt are power of incident and transmitted EM waves respectively. As, the Pt is always less than Pi, therefore, SE is a negative quantity such that a shift towards more negative value means increase in magnitude of SE. It is important to note that the losses associated with multiple reflections can be ignored (SE_M~0) in all practical cases when achieved SE_T is more than -10dB. Therefore, SE_T can be expressed as (equation II)

$$SE_T(dB) =SE_R+SE_A\text{……..(II)}$$

Figure 6 shows the EM SE of CFoam C1, C2 and C3 in the X-band (8.2 to 12.4 GHz) frequency region. It is observed that SE_T is almost constant throughout the X-band frequency range in all the three types of CFoam. While the reflection component in the form of losses are varies with frequency. The SE is the average data of 201 points from 8.2 to 12.4 GHz of the different CFoams. The average value of SE_T for CFoam C1 is -22.3 dB while in case of CFoam C2 and C3, it increases to -45.7 and -48.5dB respectively. It is interesting to note that in CFoam C2 and C3, the observed SE_T is more than double to that of CFoam C1. In case of CFoam C1, the SE_T is equally shared by both reflection and absorption losses. While in case Fe_3O_4 coated CFoam C2, SE_T is governed by absorption losses (-34.3 dB) and partially shared by reflection losses (SE_R=11.3 dB). While in Fe_3O_4-ZnO coated CFoam C3, the presence of ZnO nano-rods along with ferrite nanoparticles further improve the absorption losses (-41.5) with effectively reducing reflection losses (-7.0 dB) and as a consequence maximum value of SE_T (48.5 dB) among the three types of CFoam. Furthermore, CFoam C3 provides higher surface and large interfacial area in comparison to CFoam C2 and C1 because of high aspect ratio of nano-rods, which further enhances the SE due to the absorption. The ZnO nanoparticles not only contribute in dielectric losses but also magnetic losses and as a result maximum absorption losses in CFoam C3.

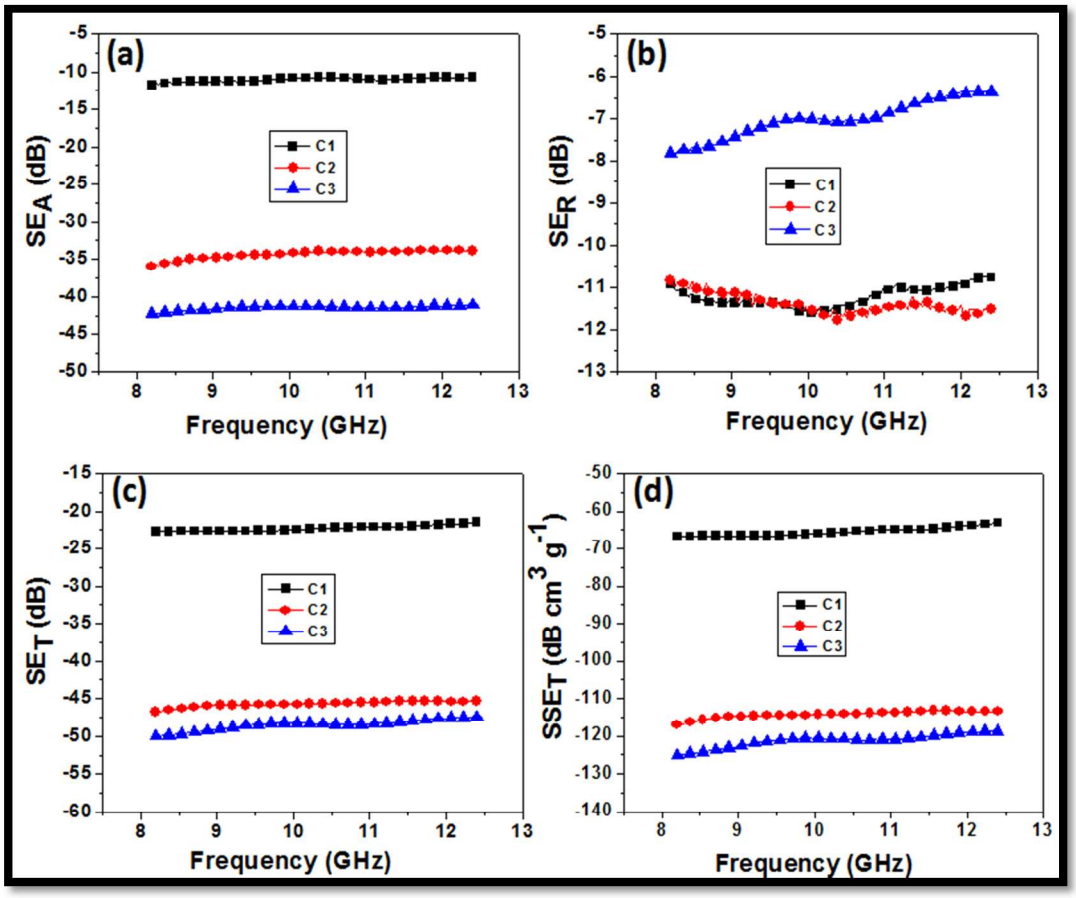

Figure 6: Electromagnetic shielding effectiveness (a) SE_A,(b) SE_R, (c) SE_T and (d) Specific SE_T of CFoam C1, C2 and C3.

In general, the SE increases with increase in conductivity but it is not always true. In our study, electrical conductivity of CFoam C2 and C3 is less than C1, but the SE is double than C1 (as discussed in the earlier section). This behaviour can be attributed to incorporation of ferrite particles of lowered complex permittivity (ε_r), and which improved the equally complex permittivity and permeability (ε_r and μ_r) of CFoam, which can help in level an impedance matching [41,45]. The Specific shielding effectiveness of CFoamC1, C2 and C3 are -66, -117 and -125dB.cm^3/g (figure 6d). This is due to the fact that the coatings of Fe_3O_4 and ZnO nanoparticles playing important role in improving magnetic and dielectric losses in the CFoam C2 and C3 which further improve the attenuation of EM radiation.

In Table 2 compared the available data on the shielding effectiveness on the CFoam, very little information ii available in open literature on CFoam as EMI shield material. From the table it is very clear that, approach adapted in this study is so for not initiated for improving the absorption of the microwave in CFoam. In most of the reported study total SE is dominated by reflection losses. The reported studies maximum absorption losses are 25 % while in present study the absorption losses more than 80% of total SE. Due to high value of the EM absorption by magnetic and dielectric nanoparticles coated CFoam, this can an excellent material for use in stealth technology.

Table 2: Comparison of Total shielding effectiveness of different CFoam

Carbon foam Processing Temp.(^{O}C)	Frequency range GHz	Thickness of material (mm)	Total shielding Effectiveness (dB)	Reflection loss (dB)	Absorption Loss (dB)	Ref.
400-800	2-18	-	-	10 dB	-	[20]
800	8.2-12.4	20	-	8-10 dB		[21]
700-760	2.45	1 to 3	-	-	-	[22]
900-1000	1-4 GHz	4.0	40	-	-	[23]
-	2-3 GHz	-		45 dB		[24]
-	400MHz-18 GHz	-	40	-	-	[25]
900	26-40 GHz	-	23	16	7	[27]
1000	8.2 -12.4	2.75	50	8	42	Present

3. Conclusions

In the summary, light weight conducting CFoam decorated with magnetic and dielectric nanoparticles are developed by simple sacrificial template technique as radar emission absorbing material. The magnetic and dielectric particles coating significantly increases the radar absorption without much enhancement in density of CFoam. The coating materials can facilitate in reducing number of defects i.e. cracks on the ligaments, which positively affect in to improvement of compressive strength by 100 %. The CFoam demonstrate excellent shielding response in the frequency range 8.2 to 12.4 GHz with absorption dominated total shielding effectiveness value of -47

dB (-37 dB absorption losses) in case Fe_3O_4coated and of -50 dB (-41.5 dB absorption losses) in case Fe_3O_4-ZnO coated CFoam. The light weight CFoams absorptivity is increases due to the decrease in electrical conductivity and increase in dielectric and magnetic losses. Thus absorptivity in CFoam increases by 236 % in Fe_3O_4 coated CFoam and 281 % in Fe_3O_4-ZnO coated CFoam as compared to uncoated CFoam. Even though ZnO is dielectric material but in the vicinity of iron oxide it will also turn in to somewhat ferromagnetic material after high temperature treatment, which can contribute both magnetic and dielectric losses as well. These studies clearly bring out the fact the even small uptake of magnetic and dielectric nanoparticles significantly influence the absorption of EM radiation in conducting CFoam. The light weight CFoam have absorption losses 80% and 20 % reflection losses, thus it can be excellent useful RAM in stealth technology in civil and military applications.

Acknowledgments

Authors are highly grateful to Director, NPL, for his kind permission to publish the results. Also thankful to Mr. Jai Tawale and Dr. K.N. Sood for doing SEM . One of the authors (Rajeev Kumar) would like to thanks CSIR for SRF fellowship.

References

1. K. Gaylor, Radar Absorbing Materials - Mechanisms and Materials, DSTO Materials Research Laboratory, Cordite Avenue, Maribyrnong, Victoria 3032**,** Australia,**1989**.
2. K.J. Vinoy, R.M. Jha, Radar Absorbing Materials: From theory to Design and Characterization; Kluwer Academic Publishers, Boston, **1996**.
3. D.D.L Chung, Journal of Mater Engineering and performance 2000, **9**, 350.
4. D.D.L. Chung, Carbon 2012, **50**, 3342.
5. X.G. Chen, Y. Ye, J.P. Cheng, J. Inorg. Mater 2011, **26**, 449.

6. J.W. Klett, A.D. McMillan, N.C. Gallego, C.A. Walls, Mater. Sci., 2004,**39**,3659.

7 .M. Inagaki, T. Morishita, A. Kuno, T. Kito, M. Hirano, T. Suwa, K. Kusakawa, Carbon, 2004,**42**, 497.

8. M. Inagaki, New Carbons: Control of Structure and Functions. Elsevier Sci. Ltd: Oxford,**2000**.

9. N.C. Gallego, J.W. Klett,.Carbon 2003,**41**,1461.

10. J.W. Klett, A.D. McMillan, N.C. Gallego, C.A.Walls, J MaterSci2004,**39**,3659.

11. M.Wang, C.Y.Wang, T.Q. Li, Z.T.Hu, Carbon2008,**46**,84.

12. D. Gaies, K.T. Faber, Carbon 2002, **40,**1137.

13. M.Wang, C.Wang, T, Li, Z. Hu, Carbon2008,**46**, 84.

14.T. Noda, M. Inagaki, S. Yamada, J. Non-cryst. Solids, 1969,**1**,285–302.

15.R. D. Klett, US Patent 3914,392, **1975**.

16. J. Klett, R. Hardy, E. Romine, C. Walls, T. Burchell, Carbon 2000,**38**, 953–973.

17. J.W. Klett, A.D. McMillan, N.G. Gallego, T.D. Burchell, C.A. Walls, Carbon 2004,**42**, 1849.

18. R. Kumar, S. R. Dhakate P.Saini and R.B. Mathur, RSC Adv.2013,**3**, 4145.

19. R. Kumar, S. R. Dhakate, T. Gupta, P. Saini, B. P. Singh and R. B. Mathur, Materials Chemistry A 2013, **1**, 5727.

20. J.Yang, Z.M. Shen, Z.B. Hao, Carbon 2004,**42**,1882-85.

21. Z. Fang, X. CaO, C. Li, H.Zhang, J.Zhang, H. Zhang , Carbon 2006,**44**(15),3348.

22. Fang Z, Li C, Sun J, Zhang H, Zhang J. Carbon 2007, **45**(15),2873.

23. F. Moglie, D. Micheli, S. Laurenzi, M. Marchetti, V.M. Primiani, Carbon 2012, **50**,1972.

24. D. Micheli, M. Marcheti, Engineering 2012,**4**,928.

25. Jesse M. Blacker, Douglas J. Merriman, Carbon foam EMI shield, US 2008/0078576 A1

26. J.M. Blacker, J.W.Plucinski, Electrically graded carbon foam, US,7,867,608 B2,2011.

27. P.P. Kuzhir, A. G. Paddubskaya,. S. A. Maksimenko, Highly porous conducting carbon foams for

electromagnetic applications, International Symposium on Electromagnetic Compatibility (EMC EUROPE), 2012(978-1-4673-0717-8/12/$31.00 ©2012 IEEE).

28. M. Saitoh, T. Yamamoto, T. Sakamoto, H. Niori, M. Chino, and M. Kobauashi, Ferroelectrics 2001, **263,** 9.

29. R. Arag´on, J. P. Shepherd, J. W. Koenitzer, D. J. Buttrey, R. J. Rasmussen, and J. M. Honig, Journal of Applied Physics 1985, **57,** 3221.

30.F. Tuinstra and J.L.Koenig, J Chemi. Phys.1970, **53**, 1126.

31. R. Kumar S.R. Dhakate, R.B. Mathur, J Mater Sci.2013, **48**, 7071.

32. B. Panigrahy, M. Aslam, D. Bahadur, Nanotechnology 2012, **23**, 115601.

33. A. C. Ferrari, J. Robertson, Physic Review B2000,**61**, 14095.

34. S.R. Dhakate, N. Chauhan, S. Sharma, J. Tawale, S. Singh, P.D. Sahare, R.B. Mathur, Carbon 2011, **49**(6), 1946.

35. O. N. Shebanova and P. Lazor,J Raman Spectro2003, **34**, 845.

36. A. M. Nicolson and G. F. Ross, IEEE Trans. Instrum Mea, 1970, **19** 377.

37. A. P. Singh, P. Garg, F. Alam, K. Singh, R. B. Mathur, R. P. Tandon, A. Chandra and S. K. Dhawan, Carbon, 2012, **50**, 3868–3875.

38. J. Wang, H. Zhou, J. Zhuang, Q. Liu, Nature Scientific Reports. 2013, **3**, 3252.

39. N. F. Colaneri and L. W. Shacklette, IEEE Trans. Instrum. Meas., 1992, 41, 29.

40. N. C. Das, D. Das, T. K. Khastgir and A. C. Chakrraborthy, Composites, Part A, 2000, 31,1069–1081.

41. A. P. Singh, M. Mishra, P. Sambyal, B. K. Gupta, B. P. Singh, A. Chandra and S. K. Dhawan, Journal of Materials Chemistry A, 2014,**2**, 3581.

42. S. Y.Bae, C.W. Na, J.H. Kang, J. Park, J. Phys. Chem. B 2005**,109**, 2526.

43. Y. Yong, M.C. Gupta, K.L. Dudley, R.W. Lawrence, Adv. Mater.2005,**17**,1999.

44. X. Han, YS Wang, J. Funct Mater devices 2007, **13**, 529.

45. B. Belaabed, J. L. Wojkiewicz, S. Lamouri, N. El Kamchi and T. Lasri, Journal of Alloys and Compounds, 2012, **527**, 137.

Figure Captions

Figure 1: SEM images of (a) Polyurethane template Foam, (b) CFoam C1, (c) CFoam C2 coated with Fe_3O_4, (d) CFoam C2 in which cracks generated after heating, (e) CFoam C3 coated with Fe_3O_4-ZnO**,** (f) ZnO nanorods generated inside the pores of CFoam C3.

Figure2: X-ray diffraction pattern of CFoam C1, C2 and C3.

Figure3: (a) Raman Spectra of CFoam C1, C2 and C3.

(b) Raman Spectra of CFoam C2 and C3 in the Raman shift range (100-900 cm^{-1})

Figure 4: (a) Real permittivity and permeability (ε′,μ′), (b) imaginary permittivity and permeability ((ε″,μ″) of CFoam C1, C2 and C3.

Figure 5: The room temperature magnetization plot of CFoams C1, C2 and C3.

Figure 6: Electromagnetic shielding effectiveness of CFoam C1,C2 &C3 (a) SE_T (b) SE_R (c) SE_A.